PCCP

Cite this: *Phys. Chem. Chem. Phys.*, 2011, **13**, 9667–9675

www.rsc.org/pccp

PAPER

Band gap anomalies of the $ZnM_2^{III}O_4$ (M^{III} = Co, Rh, Ir) spinels

David O. Scanlon* and Graeme W. Watson*

Received 16th November 2010, Accepted 24th March 2011
DOI: 10.1039/c0cp02562c

Development of high figure-of-merit p-type transparent conducting oxides has become a global research goal. $ZnM_2^{III}O_4$ (M^{III} = Co, Rh, Ir) spinels have been identified as potential p-type materials, with $ZnIr_2O_4$ reported to be a transparent conducting oxide. In this article the geometry and electronic structure of $ZnM_2^{III}O_4$ are studied using the Perdew-Purke-Ernzerhof generalized gradient approximation (PBE-GGA) to density functional theory and a hybrid density functional, HSE06. The valence band features of *all* the spinels indicate that they are not conducive to high p-type ability, as there is insufficient dispersion at the valence band maxima. The trend of increasing band-gap as the atomic number of the M^{III} cation increases, as postulated from ligand field theory, is not reproduced by either level of theory, and indeed is not seen experimentally in the literature. GGA underestimates the band-gaps of these materials, while HSE06 severely overestimates the band-gaps. The underestimation (overestimation) of the band-gaps by GGA (HSE06) and the reported transparency of $ZnIr_2O_4$ is discussed.

I. Introduction

Transparent conducting oxides (TCOs) represent an important class of materials in the field of optoelectronics,[1] possessing the normally mutually exclusive properties of transparency to visible light (optical band-gaps greater than 3.1 eV) and high conductivity (carrier concentrations of at least 10^{20}cm^{-3}, with conductivities of the order of 10^4 S cm^{-1}). TCOs have found applications in solar cells, flat panel displays, invisible security circuits *etc*.[2] One of the major limitations in developing the field of TCO research is the paucity of effective p-type materials, as a p-type TCO with conductivity comparable with the high performance n-type TCOs would open up the possibility of *transparent electronics*.[3] *All* of the current industry standard TCOs are n-type (*e.g.* SnO_2:F,[4] In_2O_3:Sn[5] and ZnO:Al),[6] but the development of a high quality p-type TCO has remained elusive.

P-type TCOs have really only been a reality since 1997, when Kawazoe *et al*. first reported simultaneous p-type conductivity and transparency in thin films of Delafossite $CuAlO_2$.[7] $CuAlO_2$ was identified as a p-type TCO using design principles[8] that subsequently were called "*chemical modulation of the valence band*". These design principles essentially combine the the valence band features of Cu_2O with the larger band gaps of other binary trivalent oxides.[8] In the Delafossite structure, the three dimensional interactions between the $3d^{10}$ electrons on neighbouring Cu^I atoms which are thought to be the reason for the relatively small band-gap of Cu_2O ($\sim$2.17 eV),[9] are altered. In $CuAlO_2$, the Cu^I–Cu^I interactions are two dimensional, resulting in a larger band-gap, and transparency.[10–12] The valence band feature of Cu_2O are still inherent in $CuAlO_2$, meaning $CuAlO_2$ retains the p-type features of Cu_2O.[7]

The pioneering study by Kawazoe *et al*. spawned an explosion of interest in Cu^I based oxides, with other Delafossites ($CuMO_2$, M = Cr, B, Sc, Y, In, Ga)[13–20] and $SrCu_2O_2$[21–24] being identified as p-type TCOs. Subsequently, however, it has become increasingly clear that *all* of these materials suffer from low conductivities[25] with most possessing indirect band-gaps, which are not ideal for optimal device performance.[26]

In 2002, Hosono and co-workers first demonstrated that the normal spinel $ZnRh_2O_4$, with Zn occupying the tetrahedral sites and Rh occupying the octahedral sites (Fig. 1) was a p-type wide band gap semiconductor.[27] It was reported to possess a band gap of 2.1 eV, and to display an electrical conductivity of 0.7 S cm^{-1} at 300 K with no intentional doping.[27] The authors concluded that the magnitude of the bandgap was mainly composed of the ligand field splitting of the occupied t_{2g}^6 and unoccupied e_g^0 levels of octahedrally coordinated Rh^{III}.[27] $ZnRh_2O_4$ has also generated interest due to its possible thermoelectric properties,[28] potential photoelectrochemical applications,[29] and its ability to be synthesized as an amorphous material.[30] Unlike Cu-based p-type TCOs, which cannot retain their O–Cu–O linear coordination whilst amorphous, the O–Rh–O octahedral network of $ZnRh_2O_4$ is preserved in an amorphous state.[30,31] Heteroepitaxial pn junctions of crystalline $ZnRh_2O_4$/ZnO,[32] and amorphous $ZnRh_2O_4$/$InGaZnO_4$[31] have been subsequently demonstrated.

A very recent investigation of the transport properties of $ZnRh_2O_4$ by Mason and co-workers has concluded that the conductivity in this material is governed by activated, small *polaron* conductivity, with a hopping energy of 0.25 eV.[33]

School of Chemistry and CRANN, Trinity College Dublin, Dublin 2, Ireland. E-mail: scanloda@tcd.ie, watsong@tcd.ie

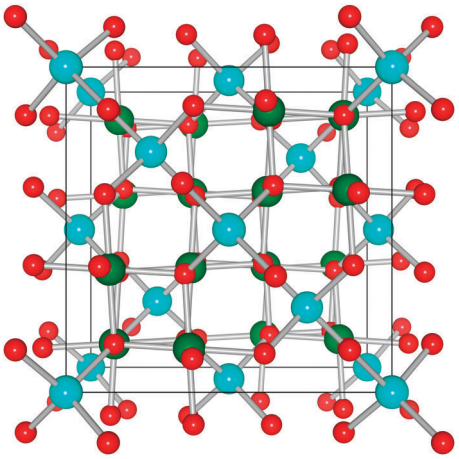

Fig. 1 Cubic spinel structure of $ZnM_2^{III}O_4$ (M^{III} = Co, Rh, Ir). The Zn atoms (turquoise) occupy tetrahedral sites and the M^{III} atoms (green) occupy octahedral sites within an fcc oxygen (red) sublattice.

This study also reported a band gap of 2.2 eV, consistent with the results of Hosono and co-workers,[27] and *not* big enough for TCO applications.[33]

Dekkers *et al.* reported the growth of p-type $ZnM_2^{III}O_4$ (M^{III} = Co, Rh, Ir) spinel thin films.[34] Based on ligand field theory,[35] Dekkers *et al.* argue that the band gaps of the spinels should increase as the principal quantum number of the d^6 element increases, meaning that band gaps will increase in the order Co 3*d* < Rh 4*d* < Ir 5*d*. This trend would also be consistent with the trend seen for the $LaM^{III}O_3$ (M^{III} = Co, Rh), where $LaRhO_2$ possesses a band gap of 1.10 eV,[36] which is greater that that of $LaCoO_3$ (0.4–0.8 eV). From optical absorption data, Dekkers *et al.* report that the band gaps of $ZnCo_2O_4$, $ZnRh_2O_4$, and $ZnIr_2O_4$ are 2.26 eV, 2.74 eV, and 2.97 eV, which conforms to their expected trends.[34] Conductivities of 0.39 S cm^{-1}(0.61 S cm^{-1}), 2.75 S cm^{-1}(2.83 S cm^{-1}) and 3.39 S cm^{-1}(2.09 S cm^{-1}) are reported for polycrystaline (epitaxial) films of $ZnCo_2O_4$, $ZnRh_2O_4$, and $ZnIr_2O_4$ respectively. In each case the conductivity displays Arrhenius-type behaviour, but with activation energies of less than 0.47m eV. To date, this is the only known report of the TCO $ZnIr_2O_4$.[34]

$ZnCo_2O_4$ is probably the most studied of the the $ZnM_2^{III}O_4$ spinels, with much interest generated due to its possible applications in gas sensing,[37,38] electrocatalysis,[39] supercapacitors,[40] Li ion batteries,[41–43] and in dilute magnetic semiconductors.[44] Kim *et al.* reported $ZnCo_2O_4$ to possess an optical band gap of 2.63 eV, and to show both *p*- and n-type conductivity depending on the oxygen partial pressure.[45] Both *p*- and n-type samples were governed by an Arrhenius behaviour, with activations energies of only 41m eV and 45m eV respectively.[45] Samanta *et al.* found that the optical band gap of $ZnCo_2O_4$ was 2.80 eV, and interestingly was of *p-d* charge transfer nature.[46]

In this article, we theoretically investigate the electronic structure of $ZnM_2^{III}O_4$ (M^{III} = Co, Rh, Ir) spinels using the PBE generalized gradient approximation approach and the state-of-the-art screened hybrid density functional, HSE06. We find that the band gap trends obtained from both the PBE and the HSE06 calculations are *not* consistent with the trend expected from ligand field theory or from the sole experimental study containing all three materials. The suitability of these Zn *d*6 spinels as p-type TCOs is discussed in light of their valence band features.

II. Calculation methodology

All DFT calculations were performed using the VASP code,[47] with the projector augmented wave (PAW)[48] approach used to describe the interactions between the core and the valence electrons. The calculations were performed using the GGA functional of Perdew, Burke and Ernzerhoff[49] (PBE) and the screened hybrid functional as proposed by Heyd, Scuseria, and Ernzerhof[50] (HSE06) in which a percentage of the exact nonlocal Fock exchange (α = 25%) is added to the PBE functional with a screening of ω = 0.11 a_0^{-1} applied to partition the exchange into long range and short range terms. Thus the exchange and correlation terms are:

$$E_{xc}^{HSE06}(\omega) = E_x^{HSE06,SR} + E_x^{PBE,LR} + E_c^{PBE} \quad (1)$$

Where

$$E_x^{HSE06,SR} = \tfrac{1}{4}E_x^{Fock,SR} + \tfrac{3}{4}E_x^{PBE,SR} \quad (2)$$

Hartree–Fock and PBE exchange are therefore only mixed in the SR part, with the LR exchange interactions being represented by the PBE functional.[50] HSE06 consistently produces structural data and band gap descriptions that are more accurate than LDA/GGA and *meta*-GGA data.[14,51–60]

Structural optimizations of the 14 atom primitive cell of the $ZnM_2^{III}O_4$ (M^{III} = Co, Rh, Ir) spinels were performed using PBE and HSE06 at a series of volumes in order to calculate the equilibrium lattice parameters. In each case the the atomic positions, lattice vector and cell angle were allowed to relax, while the total volume was held constant. The resulting energy volume curves were fitted to the Murnaghan equation of state to obtain the equilibrium bulk cell volume.[61] This approach avoids the problems of Pulay stress and changes in basis set which can accompany volume changes in plane wave calculations. Convergence with respect to *k*-point sampling and plane wave energy cut off was checked, and for both systems a cutoff of 400 eV and a Γ centered *k*-point sampling of 10 × 10 × 10 were found to be sufficient. Calculations were deemed to be converged when the forces on all the atoms were less than 0.01 eV $Å^{-1}$. The optical transition matrix elements and the optical absorption spectrum were calculated within the transversal approximation.[62] Within this methodology, the adsorption spectra is summed over all direct VB to CB transitions and therefore ignores indirect and intraband adsorptions.[63] Within this framework of single particle transitions, the electron-hole correlations are not treated, and so would require treatment by higher order electronic structure methods.[64,65]

III. Results

A. Structure

The PBE and HSE06 calculated structural paramaters for $ZnM_2^{III}O_4$ (M^{III} = Co, Rh, Ir) are given in Table 1. For $ZnCo_2O_4$ and $ZnRh_2O_4$, the PBE calculated lattice parameters are all overestimated compared to the experimental values,

whereas the HSE06 lattice parameters are underestimated. This overestimation by PBE is well known.[66] HSE06 usually predicts structural data that is more consistent with experimental values than the GGA/LDA approaches, and has been shown previously to result in underestimated lattice parameters.[57] The bond distances for $ZnRh_2O_4$ show good agreement with experimental values.[67]

The lattice parameters are seen to increase as the principal quantum number of the d^6 element increases, for both PBE and HSE06. This is to be expected when one considers the ionic radius of the d^6 cations involved, *e.g.* Co (68.5 pm) < Rh (80.5 pm) < Ir (82 pm).[69] The HSE06 calculations predict the lattice parameter of $ZnIr_2O_4$ to be 8.59 Å, which is larger than that proposed by Dekkers *et al.* for $ZnIr_2O_4$ thin films grown on Al_2O_3 (8.50 Å) or on Quartz (8.51 Å).[34] The study by Dekkers *et al.*,[34] however, reports lattice vectors for $ZnCo_2O_4$ (8.08 Å) and $ZnRh_2O_4$(8.48 Å) that are underestimated compared to other experimental values,[67,68] indicating that our HSE06 predicted value for $ZnIr_2O_4$ is reasonable.

B. PBE calculated electronic structure

The PBE calculated band structures of $ZnM_2^{III}O_4$ (M^{III} = Co, Rh, Ir) along the high symmetry lines taken from Bradley and Cracknell[70] are shown in Fig. 2(a–c). The valence band maximum (VBM) for all three spinels is located at the X point. The conduction band minimum (CBM) for $ZnCo_2O_4$ and $ZnRh_2O_4$ is located near the X point, on the line from X to Γ. Previous LDA and LDA + U calculations of $ZnRh_2O_4$ have also found that the CBM is displaced from X in the X–Γ direction,[29,33] in good agreement with the present calculations. The VBM, however, was found to be located close by the X position, shifted along the X–Γ direction using LDA + U,[33] but LDA calculations placed the VBM at the X point,[29] consistent with our PBE calculations. In contrast to this, the CBM for $ZnIr_2O_4$ is located at Γ, and is actually found to be made up of by Ir *s* and Zn *s* states, as illustrated in Fig. 3 and not Ir 5*d* states as predicted by ligand field theory. Fig. 3 clearly shows the positioning of the M^{III} *s* states in the conduction band, with the M^{III} *s* states becoming lower in energy as you go down the group. This explains the discrepancy of the CBM position for $ZnIr_2O_4$ compared to the other two materials.

The fundamental band gaps for all three materials are indirect, measuring 0.57 eV, 0.80 eV and 0.48 eV for $ZnCo_2O_4$, $ZnRh_2O_4$ and $ZnIr_2O_4$ respectively. The calculated fundamental indirect band gaps reported for $ZnRh_2O_4$ in the literature are 0.65 eV (LDA),[29] 0.81 eV (GGA)[29] and 1.65 eV (LDA + U).[33] The GGA indirect band gap reported by Singh *et al.* is 0.01 eV bigger than our calculated band gap, but this slight discrepancy can be accounted for by the fact that this value derives from a calculation at the *experimental* lattice parameters, and not at the calculated equilibrium structures as is the case in the present study. It is interesting to note the flat (non-disperse) nature of the bands around the VBM for all the spinels (Fig. 2), which are not indicative of a good p-type conductor.[33]

Fig. 4(a–c) shows the PBE calculated total and partial (ion decomposed) electronic densities of states (EDOS/PEDOS) for $ZnM_2^{III}O_4$ (M^{III} = Co, Rh, Ir). The main valence band features of all three of the spinels are broadly similar to available XPS/PES studies in the literature,[34] although the width of the PBE calculated valence bands is smaller than those seen experimentally, which is a known PBE underestimation.[15,20,71–73] In each case three distinct regions are noticeable in the valence band, region I (−9 to −6eV), region II (−6 to −2eV) and region III (−2 to 0 eV), Fig. 4(a–c). Region IV represents the lower conduction band.

Region I in each spinel is dominated by Zn *d* states with significant mixing with O 2*p* states. Region II is mainly comprised of O 2*p* states with some minor contributions from M^{III} *d* and Zn 3*d* states. Region III is seen to be split-off from the lower valence band, and is clearly dominated by M^{III} *d* states, with a small oxygen contribution. The M^{III} peaks are centered at ∼−0.8 eV, ∼0.7 eV and ∼−0.5 eV for $ZnCo_2O_4$, $ZnRh_2O_4$ and $ZnIr_2O_4$ respectively. The lower conduction band (Region IV) is also dominated by M^{III} *d* states with the main peak centered at ∼1 eV, ∼1.8 eV and ∼2.2 eV for $ZnCo_2O_4$, $ZnRh_2O_4$ and $ZnIr_2O_4$ respectively.

C. HSE06 calculated electronic structure

Fig. 5 shows the HSE06 calculated band structure of $ZnM_2^{III}O_4$ (M^{III} = Co, Rh, Ir). The VBM of $ZnCo_2O_4$ is situated near W in the W–L direction, which is different to the PBE VBM positioning at the X point. The VBM of $ZnRh_2O_4$ and $ZnIr_2O_4$ are found to be at X and Γ respectively, which is consistent with the PBE positioning. The CBM of $ZnCo_2O_4$ and $ZnRh_2O_4$ are situated near X on the X–Γ line, with the CBM of $ZnIr_2O_4$ situated at Γ, similar to the PBE calculations, and is again found to be made up of Ir *s* and Zn *s* states, similar to the PBE calculations.

In agreement with the PBE calculations, the fundamental band gaps of all three spinels are found to be indirect, and measure 3.86 eV, 2.87 eV and 2.45 eV for $ZnCo_2O_4$, $ZnRh_2O_4$ and $ZnIr_2O_4$ respectively. The main features of the band-structure are largely unchanged, except for the much larger splitting between the valence band and conduction band. The bands at the VBM still have very little dispersion, indication poor p-type ability.

Table 1 Table comparing the PBE and HSE06 calculated lattice parameters, volume, Zn–O and d^6–O interatomic distances with experimental results. Volumes are given in $Å^3$ and lattice dimensions and interatomic distances in Å

	$ZnCo_2O_4$			$ZnRh_2O_4$			$ZnIr_2O_4$		
	PBE	HSE06	Expt[68]	PBE	HSE06	Expt[67]	PBE	HSE06	Expt[34]
a	8.17	8.01	8.10	8.57	8.48	8.54	8.75	8.59	8.51
Volume	546.1	514.5	531.4	631.2	611.7	622.8	671.1	634.3	615.6
Zn–O	1.98	1.94	—	2.00	1.98	2.05	2.07	2.01	—
d^6–O	1.93	1.89	—	2.01	2.04	2.03	2.09	2.06	—

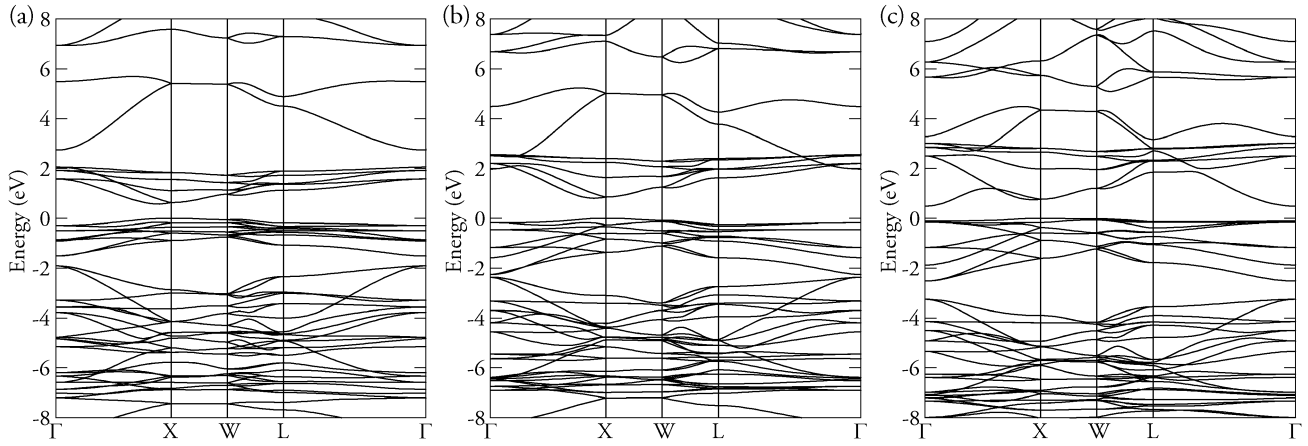

Fig. 2 PBE calculated band structures for (a) $ZnCo_2O_4$, (b) $ZnRh_2O_4$, and (c) $ZnIr_2O_4$. The VBM is set to 0 eV in each case.

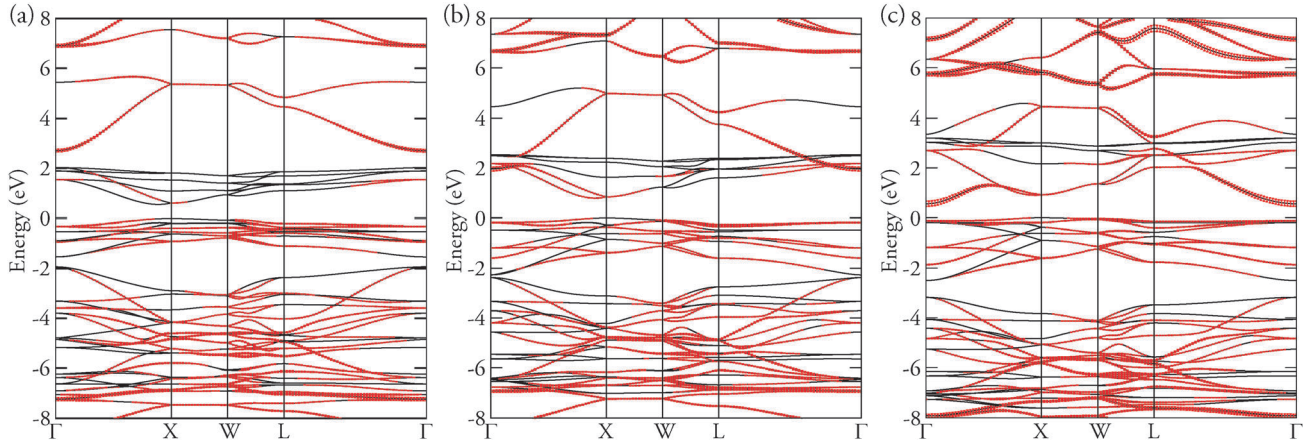

Fig. 3 PBE calculated fat band analysis for (a) $ZnCo_2O_4$, (b) $ZnRh_2O_4$, and (c) $ZnIr_2O_4$, showing the contributions of the M^{III} *s* states to the band structure. The VBM is set to 0 eV in each case.

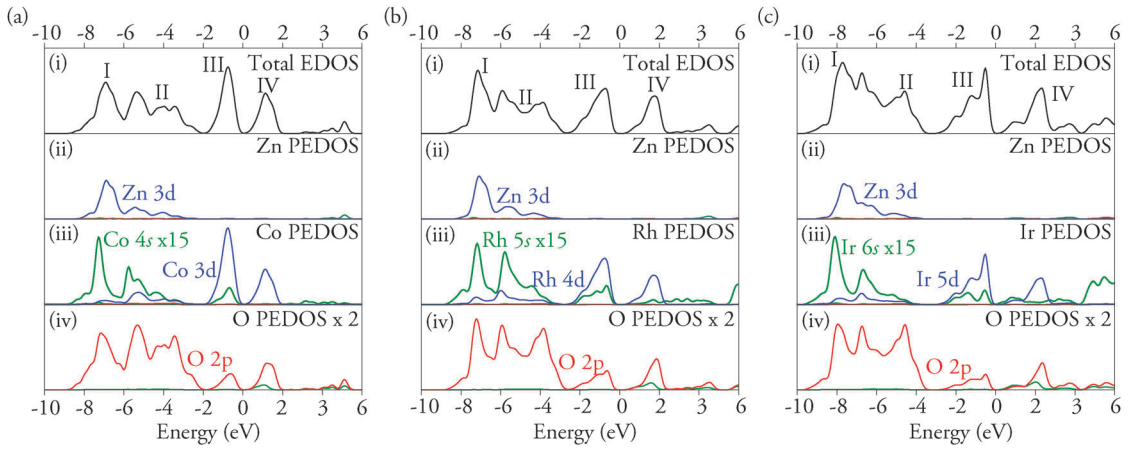

Fig. 4 The PBE electronic density of states for (a) $ZnCo_2O_4$, (b) $ZnRh_2O_4$ and (c) $ZnIr_2O_4$. (*i*) Total EDOS, (*ii*) Zn PEDOS, (*iii*) M^{III} PEDOS and (*iv*) O PEDOS. The blue lines represent *d* states, green *s* states and red *p* states.

The HSE06 calculated total and partial (ion decomposed) electronic densities of states (EDOS/PEDOS) for $ZnM_2^{III}O_4$ (M^{III} = Co, Rh, Ir) are shown in Fig. 6(a–c). The EDOS and PEDOS of the individual spinels are very similar to those obtained with the PBE functional. The major differences are (i) the peak positioning in Region I, where the Zn *d* states are pushed to lower energies relative to the VBM than in the PBE PEDOS, and (ii) the splitting of the occupied and unoccupied manifolds of the M^{III} states is appreciably increased. Overall the shapes of the peaks remain unchanged.

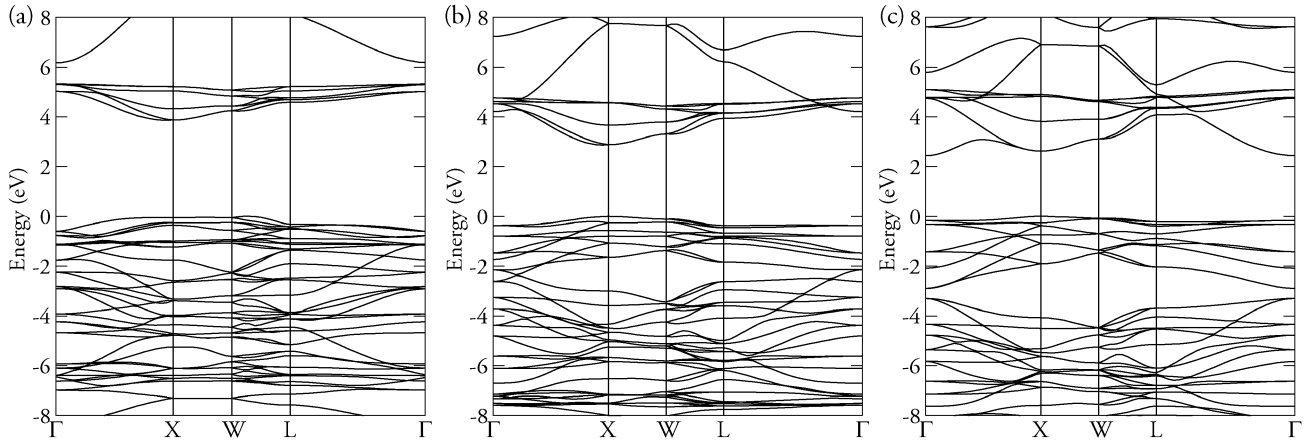

Fig. 5 HSE06 calculated band structures for (a) $ZnCo_2O_4$, (b) $ZnRh_2O_4$, and (c) $ZnIr_2O_4$. The VBM is set to 0 eV in each case.

Comparing the HSE06 valence band features with the PES data from the literature, it is noticeable that the peak associated with the Zn *d* states is closer to the experimental position than that obtained using PBE. Experimentally, the Zn 3*d* peaks are reported to occur at ~−8.8 eV, ~−9.2 eV and ~−9.5 eV for $ZnCo_2O_4$, $ZnRh_2O_4$ and $ZnIr_2O_4$ respectively.[34] The HSE06 calculations place these peaks at ~−6.8 eV, ~−7.8 eV and ~−9 eV for $ZnCo_2O_4$, $ZnRh_2O_4$ and $ZnIr_2O_4$ respectively. The corresponding PBE peak positions are ~−7 eV, ~−7.2 eV and ~−7.8 eV respectively, Fig. 4(a–c). GGA has long been known to incorrectly position occupied Zn *d* states compared to experiment[74] due to the inherent self interaction error, with HSE06 improving the positioning of these states.

IV. Discussion

The PBE fundamental band gap trend of $ZnRh_2O_4$ (0.80 eV) > $ZnCo_2O_4$ (0.57 eV) > $ZnIr_2O_4$ (0.48 eV) is *not* the trend expected from ligand field theory.[35] The splitting of the occupied t_{2g}^6 and unoccupied e_g^0 states in an octahedral field is expected to increase on going down the group,[35] and as the M^{III} *d* manifolds are expected to dominate the top of the VB and the bottom of the CB, the band gaps of these spinels are expected to follow this trend.[34] The HSE06 calculations indicate that the fundamental band gaps of $ZnCo_2O_4$, $ZnRh_2O_4$ and $ZnIr_2O_4$ are 3.86 eV, 2.87 eV and 2.45 eV respectively, which are a complete reverse of the expected trend. It should be noted, however, that band gaps for solids generally decrease as you go down a group (*e.g.* AlN > GaN > InN) due to the increase of the lattice constant. This effect does not effect the splittings of octahedral clusters of d^6 cations (*e.g.* $[M^{III}(NH_3)_6]^{3+}$(M^{III} = Co, Rh, Ir)),[75] but it might play a role in this case. The expectation, however, is that the effect of the expected increase of the band gap due to the *d–d* splitting should be much greater than any decrease in band gap due to increasing lattice constants.

The PBE (HSE06) calculated fundamental band gaps for $ZnM_2^{III}O_4$ (M^{III} = Co, Rh, Ir) are significantly smaller (larger) than those expected based on optical absorption data from the literature.[34] It should, however, be pointed out that *fundamental* band gaps are not always equivalent to *optical* band gaps. This point is very evident in the case of In_2O_3, which has an optical band gap of ~3.6 eV, yet possesses a fundamental band gap of only ~2.8 eV.[5] Similar symmetry forbidden VB–CB transitions have also been noted for SnO_2, TiO_2, Cu_2O, and $SrCu_2O_2$.[24] To fully understand the optical band gaps of these spinel materials, we have calculated the optical absorption spectra for the three materials using PBE and HSE06, with the resulting spectra displayed in Fig. 7. Analysis of the optical transitions occuring in $ZnM_2^{III}O_4$ using PBE and HSE06 reveal that the lowest *direct* transitions occur at the X point for $ZnCo_2O_4$ and $ZnRh_2O_4$, with the lowest transition in $ZnIr_2O_4$ occuring at the Γ point, with transitions from highest VB to lowest CB being symmetry allowed. The PBE trend in order of increasing optical band gaps is $ZnCo_2O_4$ < $ZnIr_2O_4$ < $ZnRh_2O_4$, which does not follow the experimentally expected trend of $ZnCo_2O_4$ < $ZnRh_2O_4$ < $ZnIr_2O_4$. HSE06 completely reverses the expected trend, producing a trend of $ZnIr_2O_4$ < $ZnRh_2O_4$ < $ZnCo_2O_4$.

In fact, the optical band gap trend expected from ligand field theory has only ever been realised in the study by Dekkers *et al.*[34] Previous experimental measurements have in fact suggested that the *optical* band gap of $ZnCo_2O_4$[45,46] is actually larger that those of $ZnRh_2O_4$.[27,33] Singh *et al.* have even predicted the band gap of $ZnRh_2O_4$ to be only ~1.2 eV.[29] Indeed the band gaps measured by Dekkers *et al.* are at variance with *all* other measurements for $ZnCo_2O_4$ and $ZnRh_2O_4$.

It is instructive to note that the performance of hybrid functionals in describing the positioning of Co 3*d* states in Co doped ZnO has been called into question by Walsh *et al.*[76] They noted that calculations using the PBE0 hybrid functional resulted in the Co *d–d* splitting being overestimated by as much as 300% compared to experiment.[76] The authors analysis showed that while 25% exchange was necessary to reproduce the experimental band gap of ZnO, less than 5% exchange was adequate for Co_3O_4. Similarily, the bandgap of $LaCoO_3$ (3.19 eV) when calculated with PBE0 is found to be in excess of 500% greater than the experimental band gap (0.6 eV).[77]

To further test the applicability of PBE and HSE06 for the description of M^{III} d^6 low spin octahedral splitting, we have also calculated the t_{2g}^6–e_g^0 splitting for $[M^{III}(NH_3)_6]^{3+}$(M^{III} = Co, Rh, Ir) octahedral complexes, Table 2. PBE underestimates the splitting for all three complexes, but maintains the experimentally reported trend of increased splitting as the principal

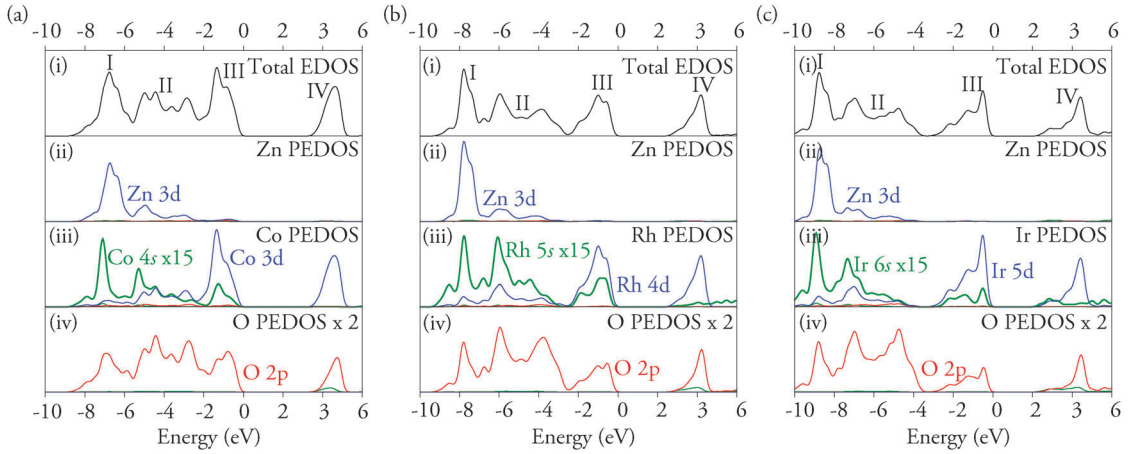

Fig. 6 The HSE electronic density of states for (a) $ZnCo_2O_4$, (b) $ZnRh_2O_4$ and (c) $ZnIr_2O_4$. (*i*) Total EDOS, (*ii*) Zn PEDOS, (*iii*) M^{III} PEDOS and (*iv*) O PEDOS. The blue lines represent *d* states, green *s* states and red *p* states.

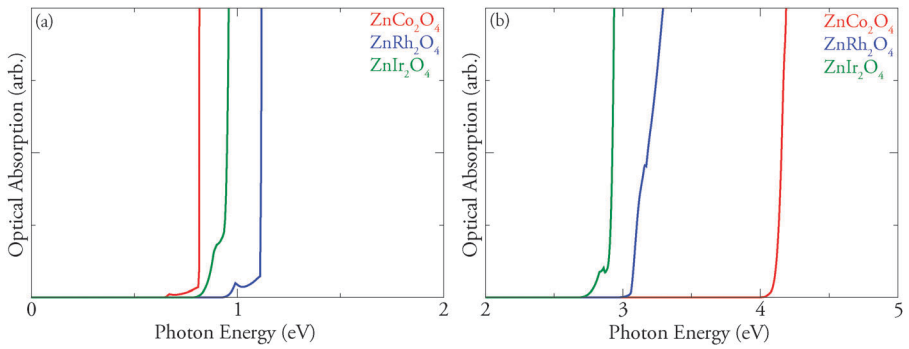

Fig. 7 (a) PBE and (b) HSE calculated optical absorption spectrum of $ZnM_2^{III}O_4$ (M^{III} = Co, Rh, Ir) summed over all possible direct valence to conduction band transitions. In both figures, $ZnCo_2O_4$ is red, $ZnRh_2O_4$ is blue and $ZnIr_2O_4$ is green.

quantum number of the M^{III} ion increases. HSE06, however, completely reverses the expected trend, and also hugely overestimates the splitting. We have also tested the ability of Hartree–Fock (HF) to describe this splitting (Table 2), and we found that it wildly overestimates the splitting of the *d* states, but also completely reverses the experimentally expected trend. The HF results are very informative, as it indicates that HF itself cannot adequately describe the splitting trend for low spin d^6 ions in an octahedral field, and it is therefore unsurprising that HSE06 cannot describe this trend.

Although there have been arguments that GGA/LDA should describe the natural octahedral splitting of these materials quite well,[29] our results indicate that PBE significantly underestimates the splitting for these spinel materials. These tests also confirm that HSE06 should be utilized with *extreme* caution when calculating binary or multiternary materials involving low spin d^6 M^{III} cations, as the accepted value of exact exchange (α = 25%) grossly overestimates the t_{2g}^6–e_g^0 splitting.

Table 2 Table comparing the GGA, HSE06 and HF calculated $t_{2g}{}^6$–$e_g{}^0$ splitting for $[M^{III}(NH_3)_6]^{3+}$ (M^{III} = Co, Rh, Ir) octahedral complexes with their experimental values. All splittings are given in eV

Material	PBE	HSE06	HF	Expt.[75]
$[Co(NH_3)_6]^{3+}$	2.61	6.24	24.51	2.85
$[Rh(NH_3)_6]^{3+}$	3.73	6.10	17.20	4.22
$[Ir(NH_3)_6]^{3+}$	4.36	6.45	16.74	5.08

Although the t_{2g}^6–e_g^0 splittings are underestimated (overestimated) with PBE (HSE), both approaches produce similar EDOS/PEDOS. There is no significant curvature at the VBM of any of the spinels, meaning that the states at the VBM are not well suited to high hole conductivity. Indeed, as the bands are clearly *not* parabolic in nature, it would not even be useful to calculate the effective hole mass of the VB. The main features of the spinels are maintained with both approaches: low lying Zn 3*d* states, with the M^{III}*d* states dominating at the top and bottom of the valence band and conduction band respectively. As the bands are flat at the VB maxima of $ZnRh_2O_4$, it is not surprising that Mason and co-workers have found that conductivity in $ZnRh_2O_4$ is polaronic in nature, with a hopping energy of 0.25 eV.[33] This is consistent with other spinels with low spin d^6 metals in the octahedral holes, which also display polaronic conductivity, *e.g.* $NiCo_2O_4$[78] and Co_3O_4.[79] Thus it is likely that $ZnCo_2O_4$ and $ZnIr_2O_4$ will also conduct with a polaronic mechanism, which is not ideal for TCO applications.

It is thus clear that the undoped $ZnM_2^{III}O_4$ (M^{III} = Co, Rh, Ir) spinels will *always* be limited by activated conductivity, and

if they are to become successfull p-type semiconductors, a change in mechanism from small polaron transort to degenerate semiconducting behaviour is necessary.[33] Allied to these intrinsic conductivity limits, the experimental uncertainty about the band gaps of these materials continues, and the nature and size of the fundamental band gap of $ZnIr_2O_4$ remains uncertain. Whether $ZnIr_2O_4$ is actually a TCO or not is still uncertain, although calculations indicate that the nature of the band gap is not solely determined by *d–d* splitting, as the CBM at the Γ point is found to be of distinct Ir *s* and Zn *s* character using both PBE and HSE06. A reinvestigation of the optical band gaps of these spinel materials is thus warranted.

At this juncture, it is instructive to pose the question, can high performance p-type TCOs be realized? It is becoming increasingly obvious that Cu(I) based TCOs based on the delafossite or $SrCu_2O_2$ structure can *never* match the high performance conductivities of n-type TCOs such as In_2O_3:Sn.[80] Delafossite materials will always be limited by deep defect levels[81] and their polaronic nature,[82–85] which is actually unsurprising when you take into account the polaronic nature of the parent compound Cu_2O,[56,86–89] which displays typical resistivities of the order of 35Ω cm.[90]

The band engineering concepts of "Chemical modulation of the valence band" can be extended to materials with other chalcogenides as the anion, and not solely oxygen.[91] Cu based chalcogenides (*e.g.* Cu_2S, Cu_2Se) possess much narrower band gaps than their oxide counterpart,[92] but have greater hole mobility due to stronger hybridization of the chalcogens with the Cu 3*d* states at the VBM. Layered oxychalcogenides, however, have emerged as attractive alternatives TCOs , as they can maintain the wide band-gaps of the oxides, allied with the increased hybridization of the chalcogen, Ch p^6 (Ch = S, Se, Te) and Cu $3d^{10}$ states at the VBM. These materials posess common $[Cu_2Ch_2]^{2-}$ layers between oxide layers with ionic cations (*e.g.* La, Sr *etc.*), with the Cu–Ch bonds forming VBMs with increased hybridization relative to the Cu–O VBMs in Cu^I based TCOs.[93]

The first layered oxychalocgenide identified as a p-type TCO was LaCuOS, which was synthesized by Hosono and co-workers in 2000.[94] This layered material possessed a band-gap of 3.1 eV and when Sr doped showed p-type conductivity of 2.6×10^{-1} S cm^{-1}.[95] Replacing the chalcogen in the structure with Se results in a p-type material with increased conductivity, but a decreased bandgap.[96] In fact Mg-doped LaCuOSe displayed a very promising conductivity of 910 S cm^{-1}, a hole concentration greater than 10^{21} cm^{-3} and a hole mobilities as high as 3.5 $cm^2V^{-1}s^{-1}$.[97] However the optical band-gap of this material is only 2.8 eV, effectively ruling it out as a possible transparent conductor.[97]

Recently $[Cu_2S_2][Sr_3Sc_2O_5]$ was found to have possess a band gap of 3.1 eV, coupled with an *undoped p*-type conductivity measured at 2.8 S cm^{-1}, which is higher than the best undoped delafossite system ($CuBO_2$, 1.65 S cm^{-1}),[57,98] and is two orders of magnitude higher than undoped LaCuOS (0.01–0.1 S cm^{-1}.[99] Interestingly, the carrier concentration in undoped $[Cu_2S_2][Sr_3Sc_2O_5]$ is relatively low at $1 \times 10^{17}cm^{-3}$,[99] which makes the high undoped conductivity relative to other Cu^I materials quite remarkable. A possible explanation for this is the *extremely* high hole mobility of $[Cu_2S_2][Sr_3Sc_2O_5]$, which at 150 $cm^2V^{-1}s^{-1}$ at room temperature, is the *largest* hole mobility of *any p*-type TCO, and *also* is *bigger* than the highest mobility reported for n-type TCOs (In_2O_3:Mo, 130 $cm^2V^{-1}s^{-1}$).[99] This illustrates, however, the ability of chalcogen anions, allied with Cu^I cations to be good candidate p-type materials. The challenge remains to engineer a layered oxychalcogenide with sufficient p-type conductivity and better transparency, to equal the performance of the n-type TCOs.

V. Conclusion

The geometry and electronic structure of $ZnM^{III}_2O_4$ (M^{III} = Co, Rh, Ir) spinels have been investigated using GGA and HSE06 functionals. GGA is found to underestimate the experimental band gap compared to experiment, wheras HSE06 is found to severly overestimate the octahedral M^{III} t^6_{2g}–e^0_g splitting compared to experiment. The exact band gap trend expected for these materials based on ligand field theory is not recreated by either method. In the case of $ZnIr_2O_4$, both GGA and HSE06 indicate that the fundamental band gap is not controlled by *d–d* splitting as was expected, but instead is *d*–M^{III}*s*. This finding calls into question the expectation that the band gap of $ZnIr_2O_4$ will be the largest of the spinels, and also the view that $ZnIr_2O_4$ is a TCO. The lack of dispersion at the VBMs of all three spinels indicates that these materials will *never* be a suitable, high performance p-type alternative to the industry standard n-type TCOs.

Acknowledgements

This publication has emanated from research conducted with financial support of Science Foundation Ireland: PI Grant Number 06/IN.1/I92 and 06/IN.1/I92/EC07. We also acknowledge support from the HEA for the PTRLI programs IITAC (Cycle III) and e-INIS (CYCLE IV). All calculations were performed on the IITAC and Lonsdale supercomputers as maintained by the Trinity Centre for High Performance Computing (TCHPC) and the Stokes computer, maintained by the Irish Centre for High-End Computing (ICHEC).

References

1 K. L. Chopra, S. Major and D. K. Pandya, *Thin Solid Films*, 1983, **102**, 1–46.
2 R. G. Gordon, *MRS Bull.*, 2011, **25**, 52–57.
3 G. Thomas, *Nature*, 1997, **389**, 907.
4 K. G. Godinho, A. Walsh and G. W. Watson, *J. Phys. Chem. C*, 2009, **113**, 439–448.
5 A. Walsh, J. L. F. Da Silva, S. H. Wei, C. Korber, A. Klein, L. F. J. Piper, A. DeMasi, K. E. Smith, G. Panaccione, P. Torelli, D. J. Payne, A. Bourlange and R. G. Egdell, *Phys. Rev. Lett.*, 2008, **100**, 167402.
6 A. F. Kohan, G. Ceder, D. Morgan and C. G. Van de Walle, *Phys. Rev. B: Condens. Matter*, 2000, **61**, 15019–15027.
7 H. Kawazoe, H. Yasakuwa, H. Hyodo, M. Kurita, H. Yanagi and H. Hosono, *Nature*, 1997, **389**, 939.
8 H. Kawazoe, H. Yanagi, K. Ueda and H. Hosono, *MRS Bull.*, 2011, **25**, 28–36.
9 J. P. Hu, D. J. Payne, R. G. Egdell, P. A. Glans, T. Learmonth, K. E. Smith, J. Guo and N. M. Harrison, *Phys. Rev. B: Condens. Matter Mater. Phys.*, 2008, **77**, 155115.
10 A. Filippetti and V. Fiorentini, *Phys. Rev. B: Condens. Matter Mater. Phys.*, 2005, **72**, 035128.

11 E. Ruiz, S. Alvarez, A. Alemany and R. Evarestov, *Phys. Rev. B: Condens. Matter*, 1997, **56**, 7189.
12 A. Buljan, M. Llunell, E. Ruiz and P. Alemany, *Chem. Mater.*, 2001, **13**, 338–344.
13 D. O. Scanlon, A. Walsh, B. J. Morgan, G. W. Watson, D. J. Payne and R. G. Egdell, *Phys. Rev. B: Condens. Matter Mater. Phys.*, 2009, **79**, 035101.
14 D. O. Scanlon, A. Walsh and G. W. Watson, *Chem. Mater.*, 2009, **21**, 4568–4576.
15 T. Arnold, D. J. Payne, A. Bourlange, J. P. Hu, R. G. Egdell, L. F. J. Piper, L. Colakerol, A. De Masi, P. A. Glans, T. Learmonth, K. E. Smith, J. Guo, D. O. Scanlon, A. Walsh, B. J. Morgan and G. W. Watson, *Phys. Rev. B: Condens. Matter Mater. Phys.*, 2009, **79**, 075102.
16 K. Ueda, T. Hase, H. Yanagi, H. Kawazoe, H. Hosono, H. Ohta, M. Orita and M. Hirano, *J. Appl. Phys.*, 2001, **89**, 1790–1793.
17 H. Yanagi, T. Hase, S. Ibuki, K. Ueda and H. Hosono, *Appl. Phys. Lett.*, 2001, **78**, 1583–1585.
18 H. Yanagi, S.-I. Inoue, K. Ueda, H. Kawazoe, H. Hosono and N. Hamada, *J. Appl. Phys.*, 2000, **88**, 4059–4163.
19 X. Nie, S. H. Wei and S. B. Zhang, *Phys. Rev. Lett.*, 2002, **88**, 066405.
20 D. Shin, J. S. Foord, D. J. Payne, T. Arnold, D. J. Aston, R. G. Egdell, K. G. Godinho, D. O. Scanlon, B. J. Morgan, G. W. Watson, E. Mugnier, C. Yaicle, A. Rougier, P. A. Glans, L. F. J. Piper and K. E. Smith, *Phys. Rev. B: Condens. Matter Mater. Phys.*, 2009, **80**, 233105.
21 X. L. Nie, S. H. Wei and S. B. Zhang, *Phys. Rev. B: Condens. Matter*, 2002, **65**, 075111.
22 A. Kudo, H. Yanagi, H. Hosono and H. Kawazoe, *Appl. Phys. Lett.*, 1998, **73**, 220–222.
23 K. G. Godinho, G. W. Watson, A. Walsh, A. J. H. Green, D. J. Payne, J. Harmer and R. G. Egdell, *J. Mater. Chem.*, 2008, **18**, 2798–2806.
24 K. G. Godinho, J. J. Carey, B. J. Morgan, D. O. Scanlon and G. W. Watson, *J. Mater. Chem.*, 2010, **20**, 1086–1096.
25 D. O. Scanlon, K. G. Godinho, B. J. Morgan and G. W. Watson, *J. Chem. Phys.*, 2010, **132**, 024707.
26 R. W. Brander, *Rev. Phys. Technol.*, 1972, **3**, 145–194.
27 H. Mizoguchi, M. Hirano, S. Fujitsu, T. Tomonari, K. Ueda and H. Hosono, *Appl. Phys. Lett.*, 2002, **80**, 1207.
28 G. B. Wilson-Short, D. J. Singh, M. Fornari and M. Suewattana, *Phys. Rev. B: Condens. Matter Mater. Phys.*, 2007, **75**, 035121.
29 D. J. Singh, R. C. Rai, J. L. Musfeldt, S. Auluck, N. Singh, P. Khalifah, S. McClure and D. G. Mandrus, *Chem. Mater.*, 2006, **18**, 2696–2700.
30 S. Narishuma, H. Mizoguchi, K. Shimizu, K. Ueda, H. Ohta, M. Hirano, H. Kamiya and T. Hosono, *Adv. Mater.*, 2003, **15**, 1409–1413.
31 T. Kamiya, S. Narushima, H. Mizoguchi, K. Shimizu, K. Ueda, H. Ohta, H. M. and H. Hosono, *Adv. Funct. Mater.*, 2005, **15**, 968–964.
32 H. Ohta, H. Mizoguchi, H. Hirano, S. Narushima, T. Kamiya and H. Hosono, *Appl. Phys. Lett.*, 2003, **82**, 823.
33 N. Mansourian-Hadavi, S. Wansom, N. H. Perry, A. R. Nagaraja, T. O. Mason, L. Ye and A. J. Freeman, *Phys. Rev. B: Condens. Matter Mater. Phys.*, 2010, **81**, 075112.
34 M. Dekkers, G. Rijnders and D. H. A. Blank, *Appl. Phys. Lett.*, 2007, **90**, 021903.
35 C. K. Jørgensen, *Modern Aspects of Ligand Field Theory*, North-Holland Pub. Co, Amsterdam, The Netherlands, 1971.
36 R. Asokamani, C. U. M. Trindah, G. Pari and S. Natarajan, *Mod. Phys. Lett. B*, 1995, **9**(11), 701–709.
37 X. Niu, W. Du and W. Du, *Sens. Actuators, B*, 2004, **99**, 405–409.
38 G. Y. Zhang, B. Guo and J. Chen, *Sens. Actuators, B*, 2006, **114**, 402–409.
39 B. Chi, J. Li, X. Yang, H. Lin and N. Wang, *Electrochim. Acta*, 2005, **50**, 2059–2064.
40 K. Karthikeyan, D. Kelpana and N. G. Renganathan, *Ionics*, 2008, **15**, 107–110.
41 C. Ai, M. Yin, C. Wang and J. Sun, *J. Mater. Sci.*, 2004, **39**, 1077–1079.
42 Y. Sharma, N. Sharma, G. V. Subba Rao and B. V. R. Chowdari, *Adv. Funct. Mater.*, 2007, **17**, 2855–2861.
43 Y. Qui, S. Yang, H. Deng, L. Jin and W. Li, *J. Mater. Chem.*, 2010, **20**, 4439–4444.
44 H. J. Kim, I. C. Song, J. H. Sin, H. Kim, D. Kim, Y. E. Ihm and W. K. Choo, *Phys. Status Solidi B*, 2004, **241**, 1553–1556.
45 H. J. Kim, I. C. Song, J. H. Sim, H. Kim, D. Kim, Y. E. Ihm and W. K. Choo, *J. Appl. Phys.*, 2004, **95**, 7387–7389.
46 K. Samanta, P. Bhattacharya, R. S. Katiyar, W. Iwamoto, R. R. Urbano, P. G. Pagliuso and C. Rettori, *Mater. Res. Soc. Symp. Proc.*, 2006, **891**, 0891.
47 G. Kresse and J. Furthmüller, *Phys. Rev. B: Condens. Matter*, 1996, **54**, 11169–11186.
48 G. Kresse and D. Joubert, *Jan*, 1999, **59**, 1758–1775.
49 J. P. Perdew, K. Burke and M. Ernzerhof, *Phys. Rev. Lett.*, 1996, **77**, 3865.
50 S. Heyd, G. E. Scuseria and M. Ernzerhof, *J. Chem. Phys.*, 2003, **118**, 8207–8215.
51 J. Heyd and G. E. Scuseria, *J. Chem. Phys.*, 2004, **121**, 1187–1192.
52 J. Heyd, J. E. Peralta, G. E. Scuseria and R. L. Martin, *J. Chem. Phys.*, 2005, **123**, 174101.
53 I. D. Prodan, G. E. Scuseria and R. L. Martin, *Phys. Rev. B: Condens. Matter Mater. Phys.*, 2006, **73**, 045104.
54 B. G. Janesko, T. M. Henderson and G. E. Scuseria, *Phys. Chem. Chem. Phys.*, 2009, **11**, 443–454.
55 J. E. Peralta, J. Heyd, G. E. Scuseria and R. L. Martin, *Phys. Rev. B: Condens. Matter Mater. Phys.*, 2006, **74**, 073101.
56 D. O. Scanlon, B. J. Morgan, G. W. Watson and A. Walsh, *Phys. Rev. Lett.*, 2009, **103**, 096405.
57 D. O. Scanlon and G. W. Watson, *Chem. Mater.*, 2009, **21**, 5435–5442.
58 J. P. Allen, D. O. Scanlon and G. W. Watson, *Phys. Rev. B*, 2010, **81**, 161103(R).
59 A. Stroppa and G. Kresse, *Phys. Rev. B: Condens. Matter Mater. Phys.*, 2009, **79**, 201201(R).
60 A. Stroppa and S. Picozzi, *Phys. Chem. Chem. Phys.*, 2010, **12**, 5405–5416.
61 F. D. Murnaghan, *Proc. Natl. Acad. Sci. U. S. A.*, 1944, **30**(9), 244–247.
62 M. Gajdos, K. Hummer, G. Kresse, J. Furthmuller and F. Bechstedt, *Phys. Rev. B: Condens. Matter Mater. Phys.*, 2006, **73**, 045112.
63 B. Adolph, J. Furthmuller and F. Beckstedt, *Phys. Rev. B: Condens. Matter*, 2001, **63**, 125108.
64 L. E. Ramos, J. Paier, G. Kresse and F. Bechstedt, *Phys. Rev. B: Condens. Matter Mater. Phys.*, 2008, **78**, 195423.
65 J. Paier, M. Marsman and G. Kresse, *Phys. Rev. B: Condens. Matter Mater. Phys.*, 2008, **78**, 121201.
66 B. J. Morgan, D. O. Scanlon and G. W. Watson, *e-J. Surf. Sci. Nanotechnol.*, 2009, **7**, 395–404.
67 F. Bertaut, F. Forrat and J. Dulac, *C. R. Acad. Sci. Fr.*, 1959, **249**, 726–727.
68 K. Krezhov and P. Konstantinov, *J. Phys.: Condens. Matter*, 1993, **5**, 9287–9284.
69 R. D. Shannon, *Acta Crystallogr., Sect. A: Cryst. Phys., Diffr., Theor. Gen. Crystallogr.*, 1976, **32**, 155–169.
70 C. J. Bradley and A. P. Cracknell, *Mathematical Theory of Symmetry in Solids*, Oxford Univeristy Press, 1972.
71 D. O. Scanlon, G. W. Watson, D. J. Payne, G. R. Atkinson, R. G. Egdell and D. S. L. Law, *J. Phys. Chem. C*, 2010, **114**, 4636–4645.
72 D. J. Payne, R. G. Egdell, D. S. L. Law, P. A. Glans, T. Learmonth, K. E. Smith, J. H. Guo, A. Walsh and G. W. Watson, *J. Mater. Chem.*, 2007, **178**, 1422–1428.
73 D. J. Payne, R. G. Egdell, A. Walsh, G. W. Watson, J. H. Guo, P. A. Glans, T. Learmonth and K. E. Smith, *Phys. Rev. Lett.*, 2006, **96**, 157403.
74 A. Janotti and C. G. Van de Walle, *Phys. Rev. B: Condens. Matter Mater. Phys.*, 2007, **76**, 165202.
75 R. Janes and E. Moore, *Metal Ligand Bonding*, Royal Soc. Chem., 2004.
76 A. Walsh, J. L. F. Da Silva and S. H. Wei, *Phys. Rev. Lett.*, 2008, **100**, 256401.
77 D. Gryaznov, R. A. Evarestov and J. Maier, *Phys. Rev. B: Condens. Matter Mater. Phys.*, 2010, **82**, 224301.
78 C. J. Exarhos, C. F. Windisch, K. F. Ferris and R. R. Owings, *Appl. Phys. A: Mater. Sci. Process.*, 2007, **89**, 9–18.

79 C. S. Cheng, M. Serizawa, H. Sakata and T. Hirayama, *Mater. Chem. Phys.*, 1998, **53**, 225–230.
80 O. N. Mryasov and A. J. Freeman, *Phys. Rev. B: Condens. Matter*, 2001, **64**, 233111.
81 J. Tate, H. L. Ju, J. C. Moon, A. Zakutayev, A. P. Richard, J. Russell and D. H. McIntyre, *Phys. Rev. B: Condens. Matter Mater. Phys.*, 2009, **80**, 165206.
82 F. A. Benko and F. P. Koffyberg, *J. Phys. Chem. Solids*, 1987, **48**, 431–43.
83 B. J. Ingram, T. O. Mason, R. Asahi, K. T. Park and A. J. Freeman, *Phys. Rev. B: Condens. Matter*, 2001, **64**, 155114.
84 B. J. Ingram, G. B. Gonzalez, T. O. Mason, D. Y. Shahriari, A. Barnabe, D. Ko and K. R. Poeppelmeier, *Chem. Mater.*, 2004, **16**, 5616–5622.
85 B. J. Ingram, B. J. Harder, N. W. Hrabe, T. A. Mason and K. R. Poeppelmeier, *Chem. Mater.*, 2004, **16**, 5623–5629.
86 J. W. Hodby, T. E. Jenkins, C. Schwab, H. Tamura and D. Trivich, *J. Phys. C: Solid State Phys.*, 1976, **9**, 1429–1439.
87 J. H. Park and K. Natesan, *Oxid. Met.*, 1993, **39**, 411–435.
88 A. Bose, S. Basu, S. Banerjee and D. Chakravorty, *J. Appl. Phys.*, 2005, **98**, 074307.
89 D. O. Scanlon, B. J. Morgan and G. W. Watson, *J. Chem. Phys.*, 2009, **131**, 124703.
90 O. M. Madelung, *Semiconductors: Data Handbook*, Springer, Berlin, 2004.
91 K. Ueda, H. Hiramatsu, M. Hirano, T. Kamiya and H. Hosono, *Thin Solid Films*, 2006, **496**, 8–15.
92 M. L. Liu, L. B. Wu, F. Q. Huang, L. D. Chen and J. A. Ibers, *J. Solid State Chem.*, 2007, **180**, 62–69.
93 S. J. Clarke, P. Adamson, S. J. C. Herkelrath, O. J. Rutt, D. R. Parker, M. J. Pitcher and C. F. Smura, *Inorg. Chem.*, 2008, **47**, 8473–8486.
94 K. Ueda, S. Inoue, S. Hirose, H. Kawazoe and H. Hosono, *Appl. Phys. Lett.*, 2000, **77**, 2701–2703.
95 H. Jiramatsu, K. Ueda, H. Ohta, M. Orita, M. Hirano and H. Hosono, *Thin Solid Films*, 2002, **411**, 125–128.
96 K. Ueda, H. Hosono and N. Hamada, *J. Phys.: Condens. Matter*, 2004, **16**, 5179–5186.
97 H. Hiramatsu, K. Ueda, H. Ohta, H. Hirano, M. Kikuchi, H. Yanagi, T. Kamiya and H. Hosono, *Appl. Phys. Lett.*, 2007, **91**, 012104.
98 M. Snure and A. Tiwari, *Appl. Phys. Lett.*, 2007, **91**, 092123.
99 M. L. Liu, L. B. Wu, F. Q. Huang, L. D. Chen and I. W. Chen, *J. Appl. Phys.*, 2007, **102**, 116108.